Available online at www.sciencedirect.com
ScienceDirect
Earth and Planetary Science Letters 256 (2007) 455–465
EPSL
www.elsevier.com/locate/epsl

Astronomical ages for Miocene polarity chrons C4Ar–C5r (9.3–11.2 Ma), and for three excursion chrons within C5n.2n

Helen F. Evans [a,*], Thomas Westerhold [b], Harald Paulsen [b], James E.T. Channell [a]

[a] *Department of Geological Sciences, PO Box 112120, University of Florida, Gainesville, FL 32611, USA*
[b] *MARUM-University Bremen, Leobener Strasse, PO Box 330 440, 28334 Bremen, Germany*

Received 3 April 2006; received in revised form 29 January 2007; accepted 1 February 2007
Available online 9 February 2007
Editor: C.P. Jaupart

Abstract

Ocean Drilling Program (ODP) Site 1092 from the sub-Antarctic South Atlantic produced a clear magnetic stratigraphy for the Late Miocene [Evans H.F., Channell, J.E.T., Upper Miocene Magnetic Stratigraphy from ODP Site 1092 (sub-Antarctic South Atlantic): recognition of cryptochrons in C5n, Geophys. Jour. Int., 153, (2003), 483–496]. Three short intervals of reverse polarity were identified within the long (~1 Myr) normal polarity subchron C5n.2n. These excursion chrons were tentatively correlated to the three "cryptochrons" identified within subchron C5n.2n from NE Pacific marine magnetic anomaly data. New oxygen isotope data from ODP Site 1092 have allowed astronomical calibration of eight polarity chron boundaries in the interval between C4Ar.1n and C5r.1n (9.3–11.2 Ma) as well as calibration of the three excursion chrons identified within C5n.2n. The new polarity chron ages in the C4Ar.1n–C5r.1n interval differ from a current (2004) timescale by up to 48 kyr. The astrochronology yields durations in the 3–4 kyr range for the three excursion chrons in C5n.2n. The relative paleointensity record from Site 1092, and hence the three excursion chrons, can be correlated to the deep-tow magnetic anomaly record from 19°S on the East Pacific Rise (EPR). Based on published correlation of the EPR deep-tow record with the sea-surface magnetic anomaly stack from the NE Pacific, the three excursion chrons do not correspond to the "cryptochrons" recognized in the NE Pacific stack.

Keywords: South Atlantic; cstrochronology; cryptochrons; magnetic stratigraphy; Miocene

1. Introduction

Ocean Drilling Program (ODP) Site 1092 was drilled in January 1998 on Meteor Rise, close to DSDP Site 704, during ODP Leg 177 in the South Atlantic. The site produced a clear magnetic stratigraphy for 4–13 Ma including the interval between C4Ar.1n and C5r.1n (Fig. 1) when sedimentation rates were ~3 cm/kyr. Four short reverse polarity intervals (excursion chrons) were identified within subchron C5n.2n [1]. This number was reduced to three due to recognition of an error in the Site 1092 composite splice, revealed by correlation of X-ray fluorescence (XRF) core scanning data, that resulted in duplication of one of the excursion zones [2].

The three "cryptochrons" in C5n.2n listed by Cande and Kent [3,4], hereafter referred to as CK92/95, originate from the work of Blakely [5] who identified three short wavelength magnetic anomalies ("tiny wiggles" in the terminology of CK92/95) within "Anomaly 5" from a stack of marine magnetic anomaly (MMA) records from the NE Pacific Ocean. The term

* Corresponding author. Tel.: +352 392 2231; fax: +352 392 9294.
E-mail address: geohelen@ufl.edu (H.F. Evans).

0012-821X/$ - see front matter © 2007 Elsevier B.V. All rights reserved.
doi:10.1016/j.epsl.2007.02.001

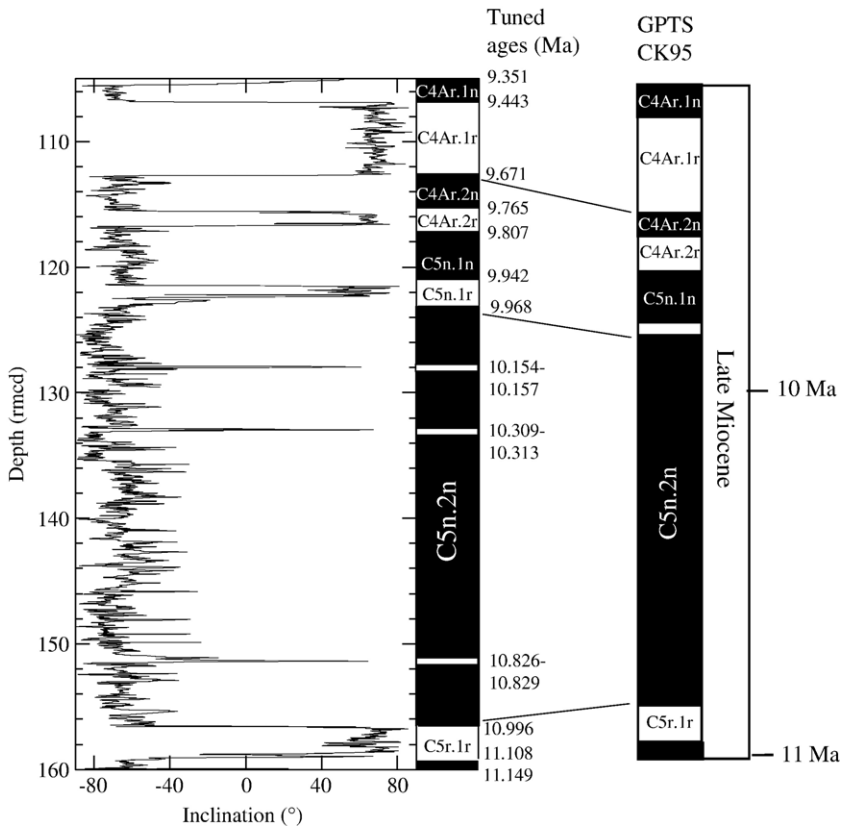

Fig. 1. Magnetic component inclination for the C4Ar.1n–C5r.1n interval from ODP Site 1092 [1] compared to the geomagnetic polarity timescale of Cande and Kent [3,4]. rmcd=revised meters composite depth [2].

"cryptochron" expresses the uncertainty in origin of these "tiny wiggles" that may be attributed to polarity excursions/chrons or fluctuations in geomagnetic paleointensity. The resolution of Blakely's [5] record did not allow precise estimation of the spacing of the short wavelength anomalies. They were placed at ~300 kyr intervals within C5n.2n, and Blakely [5] attributed these short wavelength anomalies to full polarity reversals of the geomagnetic field. These polarity subchrons within C5n.2n were included in some subsequent timescales including those of Ness et al. [6] and Harland et al. [7,8], but were relegated to "cryptochrons" in CK92/95.

In the last decade, CK92/95 has been the standard polarity timescale used in the vast majority of studies that involve the integration of magnetic, bio- and chemo-stratigraphies. The timescale was constructed by deriving a composite geomagnetic polarity sequence from marine magnetic anomaly spacings. In the 0–5 Ma interval, CK95 used astrochronologically-derived numerical ages for polarity chrons available at the time [9,10]. Beyond 5 Ma, using the assumption of smoothly varying spreading rates, a spline function was used to fit 8 radiometric age calibration points, in the 14.8–84.0 Ma interval, to the Late Cretaceous–Cenozoic polarity record.

Since the publication of CK92/95, the astrochronological calibration of the polarity timescale has been extended beyond the last 5 Myr. The majority of these developments have been incorporated into the recently published ATNTS2004 timescale of Lourens et al. [11]. For the Late Miocene, these authors used a blend of previously published astronomical timescales [12–14] adjusted to the latest astronomical solutions [15]. This adjustment resulted in minor modification of the ages of the reversal boundaries from those given in the primary publications.

For the polarity chrons in the C4Ar.1r–C4Ar.3r interval, Lourens et al., [11] utilized records from the Mediterranean [13], and from Monti dei Corvi (northern Italy) [14]. At Monti dei Corvi, Hilgen et al. [14] tuned a cyclic alternation of marls, marly limestones and organic-rich beds to the 65°N summer insolation time-series [16]. This allowed astronomic calibration of

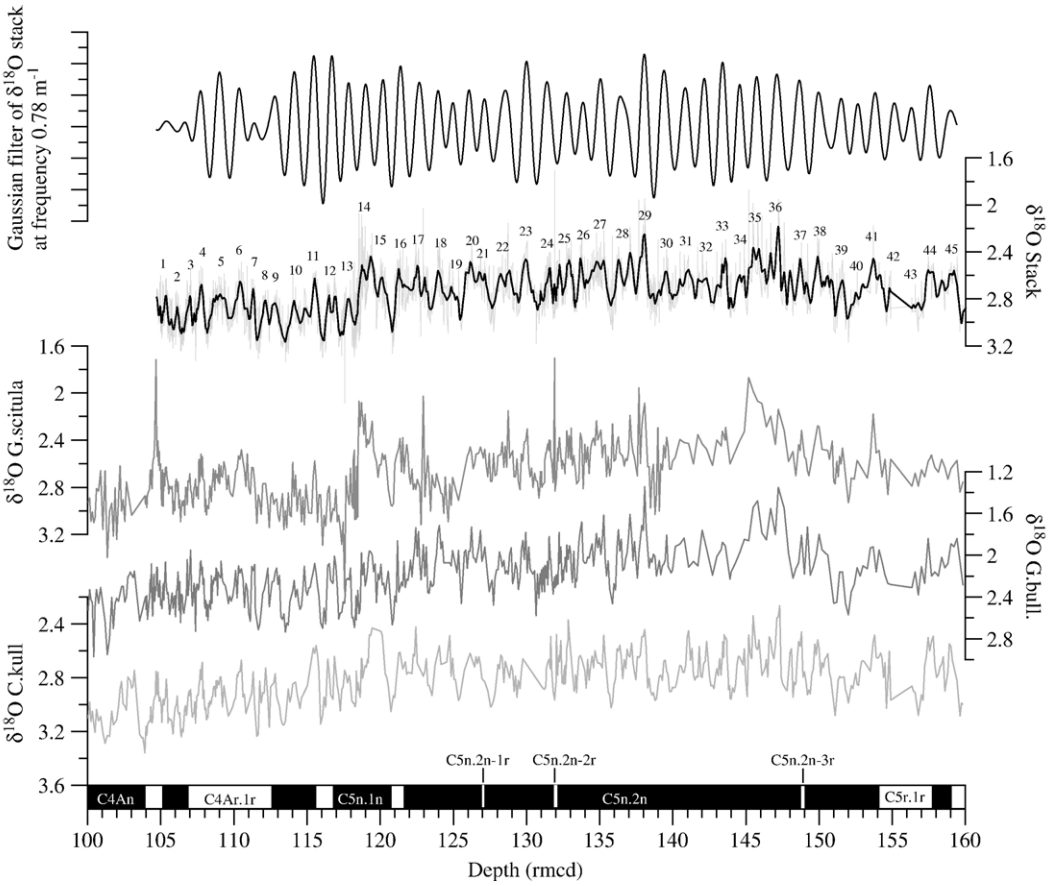

Fig. 2. Oxygen isotope records from the C4An–C5r.1n interval at ODP Site 1092. The top frame shows the output of a gaussian filter centered at a frequency of 0.78 m^{-1} applied to the stacked $\delta^{18}O$ record. The stacked $\delta^{18}O$ record with numbered obliquity cycles is shown superimposed on the same record with a 5-point smoothing. The three $\delta^{18}O$ records from different planktic and benthic foraminiferal species were used to generate the stack.

polarity chrons in the interval from C4An to the young end of C5n.2n. In the C5n.2n–C5Ar interval, Lourens et al. [11] incorporated the work of Abdul Aziz et al. [12] from the lacustrine Orera section in Spain. This section produced a reliable magnetic stratigraphy from the onset of C5n.2n to C5Ar.2n. The astronomic calibration of the reversal boundaries was accomplished using the cyclic alternation of mudstones and dolomitic carbonates identified in the sequence.

In this study, we use new oxygen isotope records from ODP Site 1092 [17] to astronomically calibrate polarity chrons C4Ar–C5r (9.3–11.2 Ma). Spectral analysis reveals a dominant obliquity (41-kyr) cycle in the oxygen isotope record and we use this to calibrate the Site 1092 record to the astronomical solution [15]. This study differs from previous astronomical timescales for this interval [12–14] in that it uses oxygen isotope records rather than lithologic cycles as the means of astronomical calibration.

2. Methods and results

At ODP Site 1092, oxygen isotope data for the Middle to Late Miocene (7–15 Ma) were generated from three species of foraminifers (Fig. 2) [17]. Benthic oxygen isotope data were generated from the benthic foraminifer *Cibicidoides kullenbergi*. Planktic oxygen isotope data were generated from two species: *Globigerina bulloides* and *Globorotalia scitula*. A power spectrum using the Blackman–Tuckey method with a Bartlett window, was generated in the depth domain from the stacked oxygen isotope record, using the Analyseries program of Paillard et al. [18] (Fig. 3a). This showed power at two frequencies: 0.78 m^{-1} and 0.25 m^{-1}. A gaussian filter centered at 0.78 (± 0.234) m^{-1} was then applied to the stacked oxygen isotope records to extract this dominant cycle. The record was then placed on an initial age model based on the magnetic stratigraphy [1] and the ATNTS2004 timescale [11]. The dominant cycle was

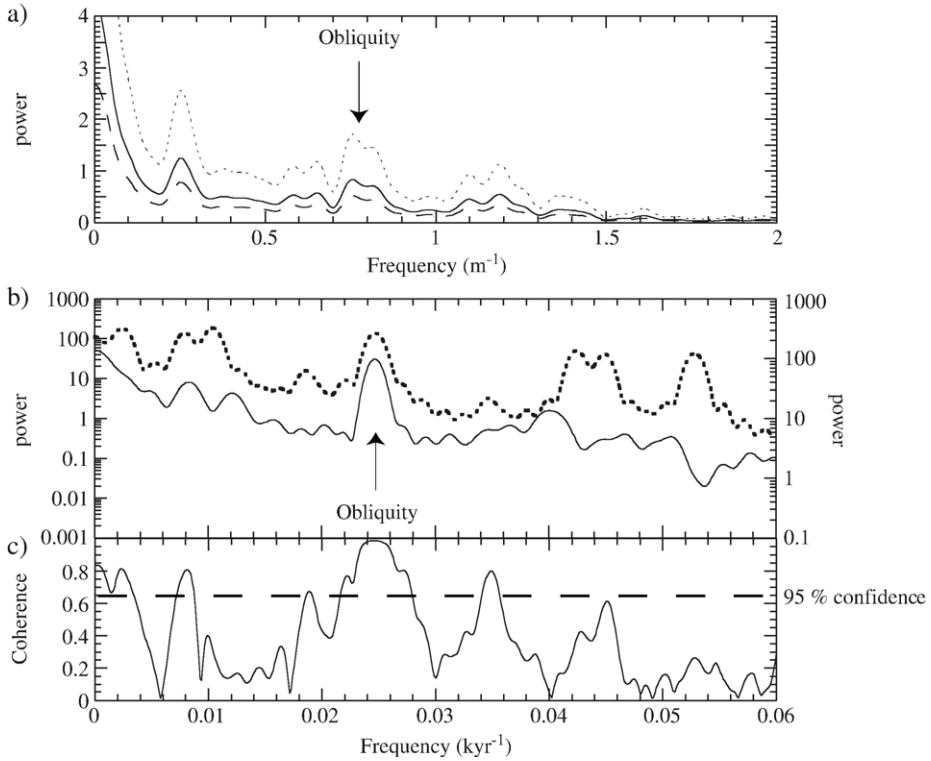

Fig. 3. a) Power spectrum generated from the oxygen isotope stack in the depth domain (solid line). b) Dashed line is the power spectrum generated from the ETP target [15] and the solid line is the power spectrum generated from the stacked oxygen isotope records after tuning. c) Coherence between the $\delta^{18}O$ stack and the ETP target curve, line indicates 95% confidence limit for coherence peaks.

identified as the 41-kyr obliquity cycle (Fig. 3b) and individual (obliquity) cycles were numbered from youngest to oldest (1–45) (Fig. 2). The second peak at a frequency of 0.25 m^{-1} (Fig. 3a) was identified as close to the 100 kyr eccentricity period.

The oxygen isotope stack was tuned to an astronomical target curve, which was derived from the sum of normalized values (minus the mean and divided by the standard deviation) of eccentricity (E), obliquity (T) and negative precession (P) ($E + T - P$) [15]. Tuning of the isotope record was only possible in the 9.3–11.2 Ma interval due to lower sedimentation rates and condensed horizons outside this interval.

For Neogene sections, it is often assumed that the 41 kyr component of $\delta^{18}O$ records is globally correlative, and not likely to be variable in phase relative to orbital forcing [19]. Much of the power in the climate spectrum since the early Oligocene appears to be concentrated in the obliquity band [20]. At Site 1092, the final age model was obtained by tuning the initial age model (from ETP tuning) until the coherence calculated using cross-spectral analysis was maximized between the filtered $\delta^{18}O$ record (filter centered at 41 kyr) and the astronomical solution for obliquity. Coherence between the oxygen isotope stack and ETP is close to one at the obliquity frequency (Fig. 3c). The 1.2 Myr modulation of the obliquity cycle is clearly visible in the filtered isotope record (Fig. 4) facilitating an unambiguous match to the orbital obliquity target. In this way, we produced an orbitally tuned age model for the 9.3–11.2 Ma interval at Site 1092.

The resulting astronomically tuned ages for C5n.2n are 44 kyr younger at the onset, and 19 kyr younger at the termination, than ages in ATNTS2004 [11]. The new ages are also significantly different from the CK92/95 ages, with the onset of C5n.2n being 47 kyr older and the termination being 48 kyr older (Table 1). Although the difference is close to one obliquity cycle, an offset by one obliquity cycle would give an inappropriate match between the $\delta^{18}O$ records and the ETP curve (Fig. 4). For example, if we shift the oxygen isotope records one obliquity cycle younger, then the light $\delta^{18}O$ values of *G. bulloides* and *C. kullenbergi* in the interval 10.78 to 10.72 Ma (Fig. 4) would be located in the ETP minimum at ~10.7 Ma which can be considered unrealistic. Interval sedimentation rates at Site 1092, calculated for

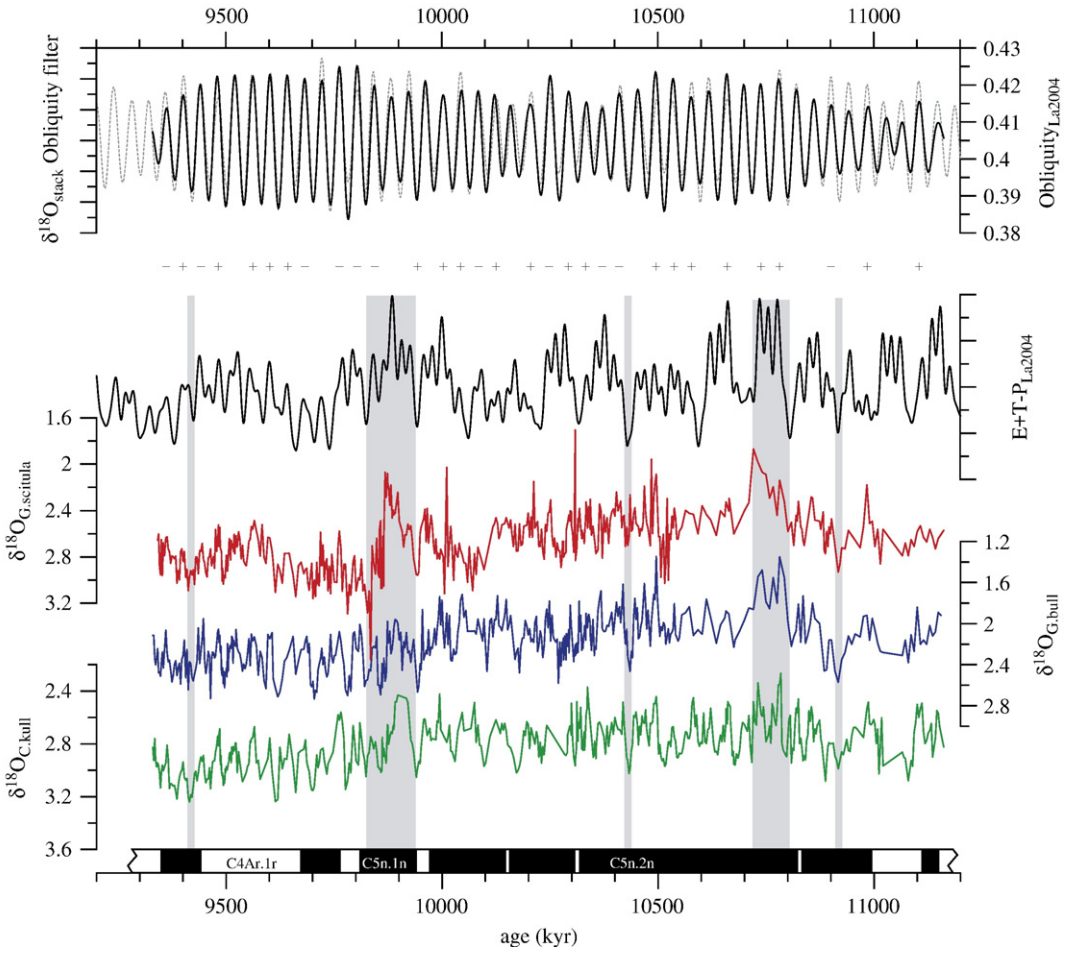

Fig. 4. Upper plot shows the correlation of the filtered (filter centered at 0.0244 ± 0.0073 kyr^{-1}) oxygen isotope stack to the astronomical solution for obliquity [15]. Lower plot shows the correlation of the three oxygen isotope records from Site 1092 to the ETP solution [15]. Crosses mark the tie points between the oxygen isotope stack and the ETP curve. Shaded areas indicate critical intervals in the correlation between the records that facilitate an unambiguous match between the oxygen isotope record and the ETP astronomic solution.

the C4Ar–C5r interval using the age-depth tie points from the tuning of the oxygen isotope records, vary from 1.7 cm/kyr to 3.7 cm/kyr for the entire interval and vary from 2.5 cm/kyr to 3.7 cm/kyr for C5n.2n (Fig. 5).

3. Errors in reversal ages

Errors in astronomically tuned reversal ages come from several sources: errors in the astronomic solution, errors in the stratigraphic placement of reversal boundaries, measurement errors associated with the response function of the u-channel magnetometer, as well as delay in remanence acquisition associated with post-depositional remanent magnetization (pDRM). The error in the astronomic solution comes from the dissipative evolution of the Earth–Moon system [15,11], and the precessional motion of the orbits of Earth and Mars [21]. The error in the Laskar et al., [15] astronomic solution, used as the tuning target in this work, is difficult to estimate due to the complex nature of the solution. Lourens et al. [11] provided an error estimate for the astronomic solution by plotting the difference (in kyr) of correlative minimum values in the obliquity and precession cycles between the $La2003_{(1,1,0)}$ and the $La2003_{(0.5,1,0)}$ solutions [15] for the last 25 Ma. The $La2003_{(1,1,0)}$ and the $La2003_{(0.5,1,0)}$ incorporate the present-day and half the present-day tidal dissipation values, respectively. At 10 Ma, the estimated error in the astronomic solution is < 20 kyr (see Fig. 21.7 of Lourens et al., [11]).

The stratigraphic depth of a reversal is taken as the depth mid-point of the polarity transition. The error in reversal depth is estimated as half the distance between the base and top of the directional transition. The stratigraphic error in reversal placement varies in the 3–

Table 1
Astronomical ages from recent timescales compared with those inferred at ODP Site 1092

Subchron	Depth (rmcd)	1092 age (ka) (errors)*	CK95 age (ka) [4]	ATNTS2004 (ka) [11]	S1995 (ka) [28]	H1995 (ka) [13]	H2000 (ka) [31]	H2003 (ka) [14]	Hu2007 (ka) [26]
Top C4Ar.1n	105.13(±0.03)	9351(±2)	9230(−121)	9312(−39)	9142(−209)			9364(+13)	9311(−40)
Base C4Ar.1n	106.96(±0.19)	9443(±10)	9308(−135)	9409(−34)	9218(−225)			9428(−15)	9426(−17)
Top C4Ar.2n	112.60(±0.05)	9671(±3)	9580(−91)	9656(−15)	9482(−189)	9629(−42)	9652(−19)	9687(+16)	9647(−24)
Base C4Ar.2n	115.60(±0.04)	9765(±2)	9642(−123)	9717(−48)	9543(−222)	9740(−25)	9762(−3)	9729(−36)	9721(−44)
Top C5n.1n	116.80(±0.05)	9807(±2)	9740(−67)	9779(−28)	9639(−168)		9841(+34)	9770(−37)	9786(−21)
Base C5n.1n	120.79(±0.05)	9942(±2)	9880(−62)	9934(−8)	9775(−167)		10,000(+58)	9871(−71)	9937(−5)
Top C5n.2n	121.61(±0.07)	9968(±2)	9920(−48)	9987(+19)	9815(−153)		10,037(+69)	10,004(+36)	9984(+16)
Top C5n.2n.1	127.00	10,154(±1)	10,197(+43)						
Base C5n.2n.1	127.09	10,157(±1)	10,205(+48)						
Top C5n.2n.2	131.96	10309 (±1)	10446 (+137)						
Base C5n.2n.2	132.10	10,313(±1)	10,470(+157)						
Top C5n.2n.3	148.83	10,826(±1)	10,710(−116)			A2003(ka)[12]			
Base C5n.2n.3	148.95	10,829(±1)	10,726(−103)						
Base C5n.2n	154.12(±0.09)	10,996(±2)	10,949(−47)	11,040(+44)	10,839(−157)	11,043(+47)	10,998(+2)		11,067(+71)
Top C5r.1n	157.71(±0.12)	11,108(±4)	11,052(−56)	11,118(+10)	10,943(−165)	11,122(+14)	11,071(−37)		11,146(+38)
Base C5r.1n	159.03(±0.03)	11,149(±1)	11,099(−50)	11,154(+5)	10,991(−158)	11,158(+9)	11,111(−38)		11,188(+39)

*Errors on Site 1092 astronomical ages take into account the uncertainty in the exact position of the magnetic reversal boundaries but not the error associated with the astronomical solution (<20 kyr at 10 Ma) or the error from a possible delay in remanence acquisition. Numbers in parentheses indicate the difference between Site 1092 estimates (this paper) and other timescales. CK95 — Cande and Kent [4], ATNTS2004 [11], A2003 — Abdul Aziz et al. [12], S1995 — Shackleton et al. [28], H1995 — Hilgen et al. [13], H2000 — Hilgen et al. [31], H2003 — Hilgen et al. [14], Hus2007 — Husing et al. [26].

19 cm range, which corresponds to 2–6 kyr based on estimated sedimentation rates (Fig. 5). The response functions of the u-channel magnetometer have a width at half-height of ~4.5 cm. Using this number, and estimated sedimentation rates, we calculate the uncertainty in age of each reversal boundary due to the finite width of the magnetometer response function as between 1.1 and 2.4 kyr. This error was mitigated by deconvolution [22] of the u-channel record across the excursional intervals [1], resulting in a modified error estimate of ~1 kyr for the C5n.2n polarity excursions. The error in reversal age associated with delayed remanence acquisition (pDRM) can be estimated by assuming that remanence lock-in occurs immediately beneath the bioturbated surface layer [23]. The lock-in depth can then be estimated from the mean sedimentation rate and the thickness of the surface bioturbated mixed-layer (~10 cm in most pelagic environments [24,25]). In the case of Site 1092, assuming a 10 cm bioturbated surface layer, the delay in remanence acquisition would be between 2.7 and 6.2 kyr depending on estimated sedimentation rate in the tuned interval (Fig. 5).

A data gap occurs in the oxygen isotope records at 155.8–157.3 revised meters composite depth (rmcd). The gaussian filter identifies two obliquity cycles in this data gap (Fig. 2). If we assume that three cycles occurred in this gap, the sedimentation rates would be anomalously low (2.3 cm/kyr), while a single cycle causes an increase in sedimentation rates (to 5.1 cm/kyr). Two obliquity cycles in this gap give sedimentation rates of 3.2 cm/kyr, consistent with adjacent intervals. The

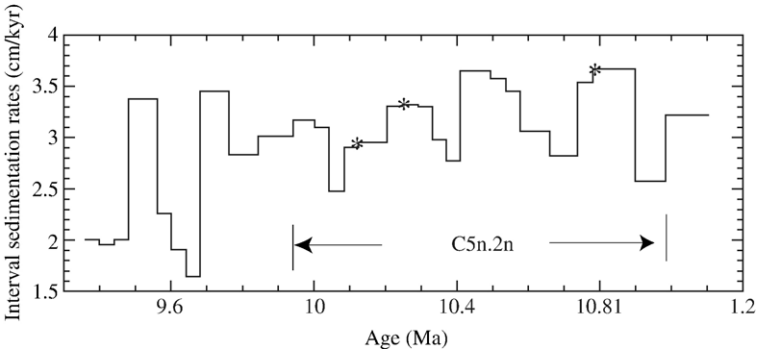

Fig. 5. Interval sedimentation rates for the C4Ar.1n–C5r.1n interval calculated using the new astrochronology. Asterisks indicate the position of polarity excursions within C5n.2n.

revised composite section is well constrained in this interval [2], and there are no indications in physical properties of a likely change in sedimentation rate.

4. Comparison with other timescales

Comparison of the new astronomical ages for subchrons C4Ar.1n to C5r.1n (9.3–11.2 Ma) with ATNTS2004 [11] reveal differences of 5–48 kyr (Table 1). A large part of the age discrepancy is probably due to the low resolution of the paleomagnetic record in the Monti de Corvi section [14] that provides the basis for the ATNTS2004 timescale in this interval. In this section, the polarity reversals are poorly defined and the pattern fit of polarity zones to polarity chrons is ambiguous, due to weak and unstable magnetic remanence. Hilgen et al. [14] gave errors of 25–77 kyr for the astronomical ages for the reversal boundaries at Monti dei Corvi, due largely to poor definition of polarity zones (see Table 3 of [14]). For C4Ar.1n–C4Ar.2n, the differences between the astronomical ages obtained at Site 1092 and those obtained at Monti dei Corvi are within these error estimates, and the differences reach 71 kyr for subchron C5n.1n where the error estimates at Monti dei Corvi are largest. Recently, Husing et al. [26] analyzed additional samples from Monti dei Corvi, and improved the placement of polarity zone boundaries. The revised polarity zone boundaries were astronomically calibrated using lithologic cycles, thereby generating revised polarity chron ages [26] (Table 1). The new astronomical ages [26] differ by up to 66 kyr from those from the previous study at Monti dei Corvi [14]. When compared to the astronomical ages from Site 1092, they differ by up to 71 kyr (Table 1).

Site 1092 and CK92/95 ages differ by ~100 kyr in the interval between C4Ar.1n and C4Ar.2n. Between the top of C5n.1n and the base of C5r.1n, the differences are 44–67 kyr (Table 1). This narrow range indicates that the durations of subchrons in this interval are very consistent between the two timescales. CK95 ages are younger than all the astronomically calibrated timescales in the 9.3–11.2 Ma interval (Fig. 6). CK92/95 relies on two calibration points for the middle to late Miocene interval. The first is placed at the older end of subchron C3n.4n with an age of 5.23 Ma from the astrochronological work of [10]. The second age calibration point at 14.8 Ma at the young end of subchron C5Bn, was derived from radioisotopic age constraints on the correlative N9/N10 foraminifer zone boundary (see [3]). According to Wei [27], this age is applicable to the N8/N9 (rather than the N9/N10) zonal boundary, possibly accounting for the relatively young ages in CK95.

Shackleton et al. [28] constructed a timescale for the Late Neogene based on gamma ray attenuation (GRA) bulk density data from sediment cores obtained during ODP Leg 138. For the 0–6 Ma interval, cycles identified in the GRA bulk density data were tuned to the orbital insolation record of Berger and Loutre [29]. The Late Miocene (6–14.8 Ma) timescale was recalibrated using two tie points at 5.875 Ma (termination of C3An) and 9.64 Ma (termination of C5n) and fitting a cubic-spline to estimate spreading rates in the manner adopted by CK92. The age control point at the termination of C5n (9.64 Ma) was generated by taking the radiometric age of 9.66+/−0.05 Ma from Baksi [30] and adjusting it to the closest age that allowed the GRA bulk density to be matched directly to the insolation record. The ages obtained by Shackleton et al. [28] are 153–225 kyr younger than those obtained for Site 1092 (Table 1). There are several possible factors that could contribute to these differences: (1) the sediment record from the ODP Leg 138 sites may not be complete in the older part, possibly attributable to use of the extended core

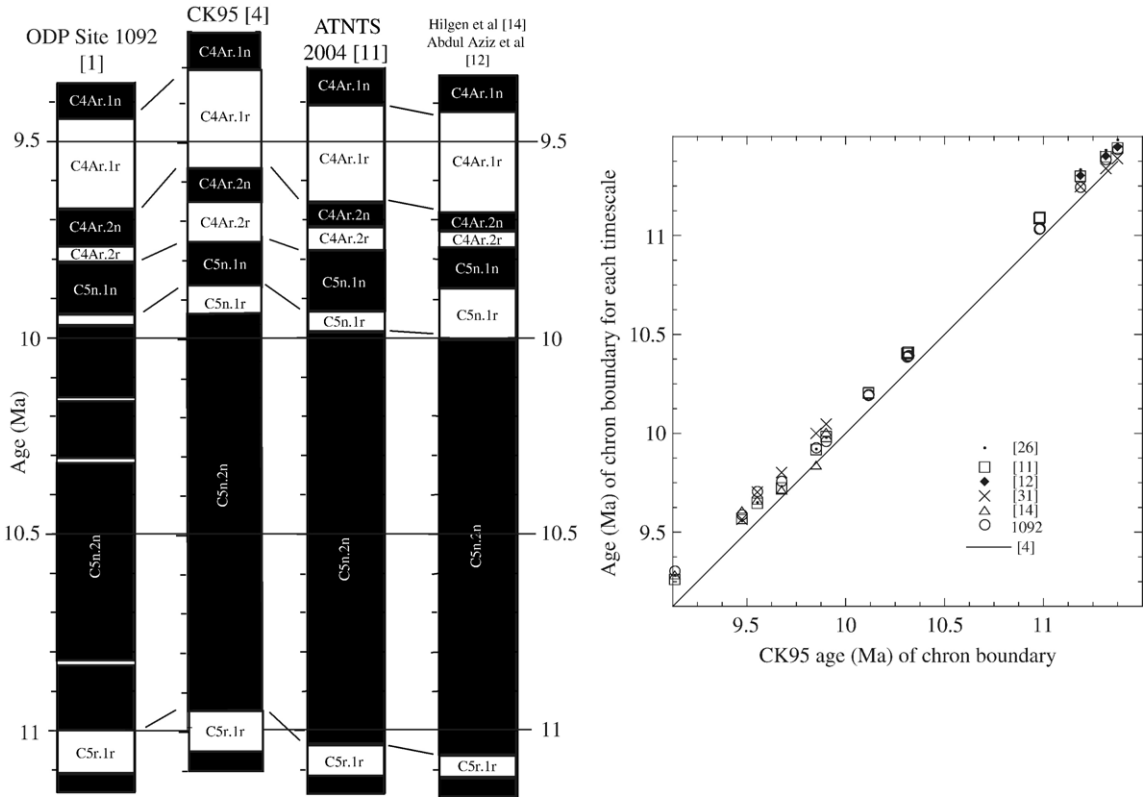

Fig. 6. Comparison of the age estimates of polarity chrons at ODP Site 1092 (this paper) to the timescale of Cande and Kent [3,4], to the ATNTS2004 timescale [11], and to the timescales of Hilgen et al. [14,31], Abdul Aziz et al. [12] and Husing et al. [26].

barrel (XCB) coring system. (2) The quality of the GRA bulk density data deteriorates, and the match to the insolation record becomes ambiguous, in the older part of the record. (3) Sedimentation rates are low (~1–2 cm/kyr) in the Late Miocene at Leg 138 sites [28].

The Monti Gibliscemi section in Sicily (Italy) is a deep marine cyclically bedded hemipelagic succession of Miocene age [31]. Due to weak magnetic intensities and overprinting, a magnetic stratigraphy was not obtained from the section. Hilgen et al. [31] indirectly estimated astronomical ages for polarity chron boundaries by transferring the astronomical ages of calcareous nannofossil events at Monti Gibliscemi to ODP Leg 138 sites in the equatorial Pacific that have reliable magnetic stratigraphies [32]. Linear interpolation of sedimentation rates between nannofossil datums yielded ages for polarity chron boundaries [31]. In the interval from C5n.1n to the base of C5n.2n, the ages from Monti Gibliscemi are consistently older than ages from Site 1092 with the mean difference being ~40 kyr (Table 1). For subchron C5r.1n, the ages are younger than those obtained in this study by 37 and 38 kyr at the young and old end of the subchron, respectively.

5. Excursion chrons

Previous estimates of the duration of polarity excursion chrons within C5n.2n from ODP Site 1092 have relied on the assumption of constant sedimentation rates within the chron [1]. Based on a mean sedimentation rate within C5n.2n of ~3 cm/kyr, the excursion chrons were estimated to have a duration of 6–11 kyr [1]. The new astronomical calibration yields durations for these excursion chrons of 3–4 kyr (Table 1).

Deep Sea Drilling Project (DSDP) Site 608 has recently yielded a revised magnetic stratigraphy for the Middle to Late Miocene [33]. Discrete samples collected every 2.5 cm at Site 608 indicate three excursions within C5n.2n, albeit represented by single samples, with estimated durations of 1–6 kyr. Three reverse polarity intervals at ODP Site 884 on the Detroit Seamount in the NW Pacific Ocean were placed within C5n.2n [34], and were calculated by the authors to have

durations of 6, 26 and 28 kyr. Ambiguities in the interpretation of the magnetic stratigraphy at Site 884, and the apparent duration of these reverse polarity intervals, makes it unlikely that they correlate to the excursional directions identified at Site 1092 (see [1]).

Roperch et al. [35] studied a 4.5 km thick middle Miocene continental red bed section in the Bolivian Altiplano. Magnetostratigraphic results indicate that the sequence was deposited during the 14–9 Ma interval, and has a mean sedimentation rate of 97 cm/kyr in the 11.5–9.2 Ma interval. Roperch et al. [35] identified one reverse polarity interval represented by five samples (at 3714–3719 m above base of section) within the normal polarity interval correlative to C5n.2n. Using an estimate for the mean sedimentation rate within C5n.2n (97 cm/kyr), this reverse interval has a duration of ~5 kyr. The Ulloma tuff lies ~100 m below the reverse polarity zone and has yielded an age of 10.35+/−0.06 Ma from $^{40}Ar/^{39}Ar$ dating of sanidine crystals [36]. Assuming a constant sedimentation rate from the top of the polarity zone correlative to C5n.2n to the Ulloma tuff the reverse polarity zone has an age of 10.21 Ma and a duration of ~8 kyr.

Bowles et al. [37] studied the sedimentary section at ODP Site 887 from the North Pacific that covers the C5n interval. The cores were sampled using discrete samples at 2.5 cm spacing. The mean sedimentation rate within C5n.2n (1 cm/kyr) implies a sampling resolution of 2500 yr, however no reverse polarity intervals were detected within C5n.2n. In view of the sedimentation rates at Site 887, it is possible that polarity intervals of the duration seen at ODP Site 1092 would not have been recorded using this sampling regime.

The Bowers et al. [38] deep-tow marine magnetic anomaly (MMA) record from the southern East Pacific Rise (EPR) (Fig. 7) is one of the most detailed MMA records for this time interval with an average half-spreading rates of 90 mm/yr. In Fig. 7, we correlate the Site 1092 paleointensity record from [1] to the deep-tow MMA record. The three brief excursion chrons observed in C5n.2n at Site 1092 can then be placed into the deep-tow MMA record (arrows from below in Fig. 7). The preferred correlation between the EPR deep-tow magnetic anomaly record and NE Pacific stack [38] shows that the Site 1092 excursion chrons do not correlate with the position of the CK92/95 “tiny

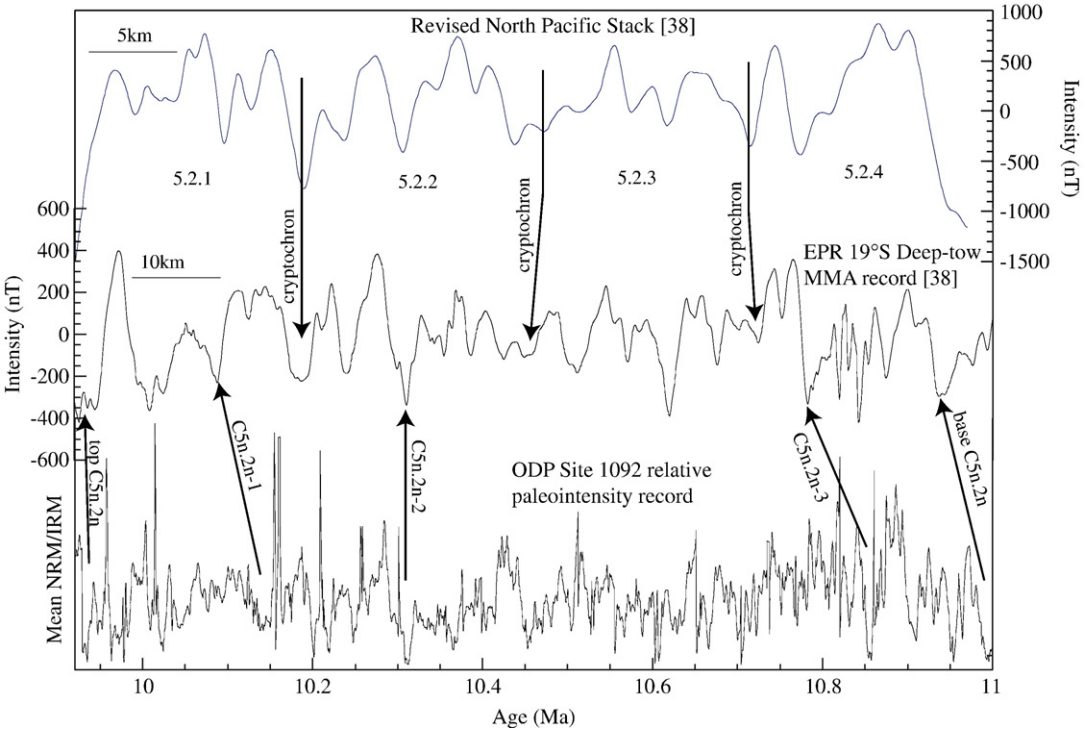

Fig. 7. The Site 1092 relative paleointensity record for C5n.2n [1] (bottom), the deep-tow magnetic anomaly record from the East Pacific Rise at 19°S (middle) and the revised North Pacific Stack [38]. Numbering on the revised NE Pacific stack is after [38]. Arrows from above indicate the proposed correlation [38] of CK92 cryptochrons to the revised N. Pacific Stack and the EPR 19°S deep-tow record. Arrows from below indicate our preferred correlation of the polarity excursion chrons to the deep-tow record.

wiggles" in sea-surface magnetic anomaly data from the NE Pacific, but do appear to correlate with magnetic features in the deep-tow record.

Oxygen isotope records from ODP Site 1092 have allowed astronomic calibration of the ages of eight polarity chron boundaries (C4Ar.1n–C5r.1n), and of three excursion chrons within C5n.2n [1,2]. This is the first time astronomically calibrated ages have been assigned to the excursion chrons within C5n.2n, and they indicate durations of 3–4 kyr. This duration estimate is consistent with the model of Gubbins [39] that predicts that excursions should have durations less than the magnetic diffusion time (3 kyr) for the inner core [40]. The duration of these excursions is less than the duration for reversal transitions such as the Matuyama–Brunhes boundary (5–10 kyr, e.g. [41]) implying that the outer core must maintain the opposite or transitional polarity state for greater than ~3 kyr to allow the outer core field to diffuse through the inner core and hence stabilize the outer core field [39]. The duration for excursions, such as those within C5n.2n, which appear as abrupt swings to reverse polarity and return to normal polarity, was apparently insufficient for establishment of a prolonged reverse polarity interval.

Acknowledgments

We would like to thank the staff at the Bremen Core Repository for assistance with sampling. Funding for this research was provided by the Deutsche Forschungsgemeinschaft as part of the DFG-Research Center 'Ocean Margins' of the University of Bremen (No. RCOM0475) to T. Westerhold and H. Paulsen, and by a Joint Oceanographic Institutions/U.S. Science Support Program (USSSP) grant to J. Channell. We also thank Steve Cande and an anonymous reviewer for comments that improved the manuscript.

References

[1] H.F. Evans, J.E.T. Channell, Upper Miocene Magnetic Stratigraphy from ODP Site 1092 (sub-Antarctic South Atlantic): recognition of cryptochrons in C5n, Geophys. J. Int. 153 (2003) 483–496.

[2] H.F. Evans, T. Westerhold, J.E.T. Channell, ODP Site 1092: revised composite depth section has implications for Upper Miocene "cryptochrons", Geophys. J. Int. 156 (2004) 195–199.

[3] S.C. Cande, D.V. Kent, A new geomagnetic polarity timescale for the late Cretaceous and Cenozoic, J. geophys. Res. 97 (1992) 13917–13951.

[4] S.C. Cande, D.V. Kent, Revised calibration of the geomagnetic polarity timescale for the late Cretaceous and Cenozoic, J. geophys. Res. 100 (1995) 6093–6095.

[5] R.J. Blakely, Geomagnetic reversals and crustal spreading rates during the Miocene, J. geophys. Res. 79 (1974) 2979–2985.

[6] G. Ness, S. Levi, R. Couch, Marine magnetic anomaly timescales for the Cenozoic and Late Cretaceous: a precise, critique and synthesis, Rev. Geophys. space phys. 18 (4) (1980) 753–770.

[7] W.B. Harland, A.V. Cox, P.G. Llewellyn, C.A.G. Pickton, A.G. Smith, R. Walters, A Geologic Time Scale, Cambridge Univ. Press, Cambridge, 1982.

[8] W.B. Harland, R. Armstrong, A.V. Cox, L. Craig, A. Smith, D.A. Smith, Geologic Time Scale 1989, Cambridge Univ. Press, Cambridge, 1990 263 pp.

[9] N.J. Shackleton, A. Berger, W.R. Peltier, An alternative astronomical calibration of the lower Pleistocene timescale based on ODP Site 677. Transactions of the Royal Society of Edinburgh, Earth Sci. 81 (1990) 251–261.

[10] F.J. Hilgen, Extension of the astronomically calibrated (polarity) time scale to the Miocene/Pliocene boundary, Earth Planet. Sci. Lett. 107 (1991) 349–369.

[11] L.J. Lourens, F.J. Hilgen, J. Laskar, N.J. Shackleton, D. Wilson, The Neogene Period, in: F.M. Gradstein, J.G. Ogg, A.G. Smith (Eds.), Geologic Time Scale 2004, Cambridge Univ. Press, 2005, pp. 409–440.

[12] H. Abdul Aziz, W. Krijgsman, F.J. Hilgen, D.S. Wilson, J.P. Calvo, An astronomical polarity timescale for the late middle Miocene based on cyclic continental sequences, J. geophys. Res. 108 (2003), doi 10.1029/2002JB001818 No. B3, 2159.

[13] F.J. Hilgen, W. Krijgsman, C.G. Langereis, L.J. Lourens, A. Santarelli, W.J. Zachariasse, Extending the astronomical (polarity) time scale into the Miocene, Earth Planet. Sci. Lett 136 (1995) 495–510.

[14] F.J. Hilgen, H. Abdul Aziz, W. Krijgsman, I. Raffi, E. Turco, Integrated stratigraphy and astronomical tuning of the Serravallian and lower Tortonian at Monti dei Corvi (Middle-Upper Miocene, northern Italy), Palaeogeogr. Palaeoclimatol. Palaeoecol. 199 (229–264) (2003).

[15] J. Laskar, P. Robutel, F. Joutel, M. Gastineau, A.C.M. Correia, B. Levrard, A long term numerical solution for the insolation quantities of the Earth, Astron. Astrophys. 428 (2004) 261–285.

[16] J. Laskar, H. Joutel, F. Boudin, Orbital, precessional and insolation quantities for the Earth from −20 Myr to +10 Myr, Astron. Astrophys 270 (1993) 522–533.

[17] H. Paulsen, Miocene changes in the vertical structure of the Southeast Atlantic near-surface water column: Influence on the paleoproductivity, Dissertation thesis, 93 pp, University Bremen, Germany, 2005.

[18] D. Paillard, L. Labeyrie, P. Yiou, Macintosh program performs time-series analysis, Trans. Am. Geophys. Union, (EOS) 77 (1996) 379.

[19] S.C. Clemens, An astronomical tuning stratigraphy for Pliocene sections: implications for global-scale correlation and phase relationship, in: N.J. Shackleton, I.N. McCave, G.P. Weedon (Eds.), Phil. Trans. R. Soc. Lond. A, 1999, pp. 1949–1973.

[20] J. Zachos, M. Pagani, L. Sloan, E. Thomas, K. Billups, Trends, Rhythms, and Aberrations in global climate 65 Ma to present, Science 292 (2001) 686–693.

[21] H. Palike, J. Laskar, N.J. Shackleton, Geologic constraints on the chaotic diffusion of the solar system, Geology, 32, No. 11, 929–932.

[22] Y. Guyodo, J.E.T. Channell, R. Thomas, Deconvolution of u-channel paleomagnetic data near geomagnetic reversals and short events, Geophys. Res. Lett. 29 (2002) 1845, doi 10.1029/2002GL014963.

[23] J.E.T. Channell, Y.J.B. Guyodo, The Matuyama Chronozone at ODP Site 982 (Rockall bank): evidence for decimeter-scale

magnetization lock-in depths, in: J.E.T. Channell, D.V. Kent, W. Lowrie, J. Meert (Eds.), Timescales of the Paleomagnetic Field, Geophysical Monograph, vol. 145, 2004.

[24] M.H. Trauth, M. Sarnthein, M. Arnold, Bioturbational mixing depth and carbon flux at the seafloor, Paleoceanography 12 (1997) 517–526.

[25] C.R. Smith, C. Rabouille, What controls the mixed-layer depth in deep-sea sediments? The importance of POC flux, Limnol. Oceanogr. 47 (2002) 418–426.

[26] S.K. Husing, F.J. Hilgen, H. Abdul Aziz, W. Krijgsman, Completing the Neogene geological time scale between 8.5 and 12.5 Ma, Earth planet. Sci. Lett. 253 (2007) 340–358.

[27] W. Wei, Revised age calibration points for the geomagnetic polarity time scale, Geophys. Res. Lett. (22) (1995) 957–960.

[28] N.J. Shackleton, S. Crowhurst, T. Hagelberg, N.G. Pisias, D.A. Schneider, A new Late Neogene time scale: application to Leg 138 sediments, Proc. ODP, Sci., Results 138 (1995) 73–101.

[29] A. Berger, M.F. Loutre, Insolation values for the climate of the last 10 million years, Quat. Sci. Rev. 10 (1991) 297–317.

[30] A. Baksi, $A^{40}Ar/^{39}Ar$ age for the termination of Chron 5; a new calibration point for the Miocene section of the GPTS, Eos 630 (73) (October 27 1992) (Suppl.).

[31] F.J. Hilgen, W. Krijgsman, I. Raffi, E. Turco, W.J. Zachariasse, Integrated stratigraphy and astronomical calibration of the Serravallian/Tortonian boundary section at Monte Gibliscemi (Sicily, Italy), Mar. Micropaleontol. 38 (2000) 181–211.

[32] D.A. Schneider, Paleomagnetism of some Leg 138 sediments: detailing Miocene magnetostratigraphy, Proc. ODP, Sci., Results 138 (1995) 59–72.

[33] W. Krijgsman, D.V. Kent, Non-uniform occurrences of short-term polarity fluctuations in the geomagnetic field? New results from Middle to Late Miocene sediments from the North Atlantic, in: J.E.T. Channell, D.V. Kent, W. Lowrie, J.G. Meert (Eds.), Timescales of the Paleomagnetic Field, AGU Geophysical Monograph, vol. 145, 2004, pp. 161–174.

[34] A.P. Roberts, J.C. Lewin-Harris, Marine magnetic anomalies: evidence that 'tiny wiggles' represent short-period geomagnetic polarity intervals, Earth planet. Sci. Lett. 183 (2000) 375–388.

[35] P. Roperch, G. Herail, M. Fornari, Magnetostratigraphy of the Miocene Corque Basin, Bolivia: implications for the geodynamic evolution of the Altiplano during the Late Tertiary, J. geophys. Res. 104 (1999) 20415–20429.

[36] L.G. Marshall, C. Swisher, A. Lavenu, R. Hoffstetter, G. Curtis, Geochronology of the mammal-bearing late Cenozoic on the northern Altiplano, Bolivia, J. South Am. Earth Sci. 5 (1992) 1–19.

[37] J. Bowles, L. Tauxe, J. Gee, D. McMillan, S. Cande, Source of tiny wiggles in Chron C5: a comparison of sedimentary relative paleointensity and marine magnetic anomalies, Geochem. Geophys. Geosyst. 4 (6) (2003) 1049, doi 10.1029/2002GC000489.

[38] N.E. Bowers, S.C. Cande, J. Gee, J.A. Hildebrand, R.L. Parker, Fluctuations of the palaeomagnetic field during chron C5 as recorded in near bottom marine magnetic anomaly data, J. geophys. Res 106 (B11) (2001) 26,379–26,396.

[39] D. Gubbins, The distinction between geomagnetic excursions and reversals 137 (1999) F1–F3 0.

[40] R. Hollerbach, C.A. Jones, On the magnetically stabilizing role of the Earth's inner core, Phys. Earth planet. Inter. 87 (1995) 171–181.

[41] J.E.T. Channell, H.F. Kleiven, Geomagnetic paleointensities and astronomical ages for the Matuyama-Brunhes boundary and the boundaries of the Jaramillo Subchron: paleomagnetic and oxygen isotope records from ODP Site 983, Phil. Trans. R. Soc. Lond. A 358 (2000) 1027–1047.